Applicability of satellite radar imaging to monitor the conditions of levees

Ozer, Ece; van Leijen, Freek; Jonkman, Sebastiaan N.; Hanssen, Ramon

DOI
10.1111/jfr3.12509

Publication date
2018

Document Version
Final published version

Published in
Journal of Flood Risk Management

Received: 29 June 2018 | Revised: 30 October 2018 | Accepted: 31 October 2018

DOI: 10.1111/jfr3.12509

CIWEM Chartered Institution of Water and Environmental Management | WILEY Journal of Flood Risk Management

ORIGINAL ARTICLE

Applicability of satellite radar imaging to monitor the conditions of levees

Işıl E. Özer | Freek J. van Leijen | Sebastiaan N. Jonkman | Ramon F. Hanssen

Faculty of Civil Engineering and Geosciences, Delft University of Technology, Delft, The Netherlands

Correspondence
Işıl E. Özer, Department of Hydraulic Engineering, Faculty of Civil Engineering and Geosciences, Delft University of Technology, Stevinweg 1, 2628 CN, Delft, The Netherlands.
Email: i.e.ozer@tudelft.nl

Funding information
Nederlandse Organisatie voor Wetenschappelijk Onderzoek

Levees are critical systems in safeguarding an area against catastrophic flooding events with potential fatalities and economic losses. Current monitoring methods of levees highly rely on expert judgement, resulting in infrequent and subjective assessments of their status. Satellite radar imaging, in particular using interferometry (InSAR), holds a large potential to monitor the condition of levees with millimetre-level precision, anywhere on the planet. However, for levee management, the usability of the technique requires significant radar expert knowledge. Here, we provide a comprehensive overview of the state of the art in using time-series InSAR for systematic levee deformation monitoring. We explore its use to complement existing approaches for assessing levee deformation and failure investigations in a fast, systematic, and cost-effective way. The applicability of imaging radar satellites is discussed, supported by case studies on levee monitoring in the Netherlands. We elaborate on the technical aspects with respect to levee monitoring using SAR technology, such as estimating deformation in different directions, satellite characteristics, precision, and reliability. We conclude that InSAR is becoming an operational deformation monitoring system, which allows for the detection, tracking, and analysis of irregularities on levee sections with increased efficiency and quality, thus contributing to improved risk management.

KEYWORDS
InSAR, levee deformation, levee monitoring, levee safety, satellite radar interferometry

1 | INTRODUCTION

Levees are critical systems that provide flood protection. Rapid economic and demographic growth, in combination with natural changes such as sea level rise, extreme weather conditions, and land subsidence, increase the potential impact of a levee failure. Consequently, failures of levees may lead to significant damage, fatalities or substantial economic, social and environmental losses. Between 1980 and 2010, 3,563 flood events occurred in Europe (of which 321 in 2010 only) and more severe floods are expected in the near future (EEA, 2018). In most cases, failure processes have not been foreseen by periodical inspections meant to assess the overall condition of levee systems. For instance, a survey of levee failures during the 2002 flood in Germany (Horlacher, Bielagk, & Heyer, 2005) and an analysis for the last 10 years of levee failures in England (Simm, Flikweert, Hollingsworth, & Tarrant, 2017) showed that the levees broke at sections that were considered to be safe according to conventional levee assessments (Heyer, 2016). Hence, many problems cannot be detected by conventional methods, making additional monitoring techniques desirable. In

addition, there are large uncertainties in the composition of levees and the behaviour during critical conditions, especially for geotechnical failure mechanisms (Schweckendiek, Vrouwenvelder, & Calle, 2014). It is therefore difficult to predict which levee sections are most vulnerable.

Frequent monitoring of the condition of levees is crucial as well as challenging. This is also the case for the Netherlands, where almost 12 million people (70% of the total population) live in flood prone areas, and 70% of the economic value produced would be endangered in case of a catastrophic event (Jorissen, Kraaij, & Tromp, 2016). Currently, the country is protected by a network of 22,500 km of flood defence structures, of which nearly 17% are primary levees protecting populated areas from flooding by major rivers, big lakes, and the sea. Hence, levee monitoring requires a considerable effort and significant financial means. The Netherlands invest over 1 billion Euro per year in activities related to monitoring, maintenance, and reinforcement of the flood defences, with the intention to maintain or increase their safety levels. However, according to a national safety report in 2014 (Vergouwe & Sarink, 2014), about 30% of these primary levees did not comply with the required safety level, which is bound to reach 50% due to the new and generally stricter safety standards introduced in 2017 (Jorissen et al., 2016).

Depending on the natural or man-induced driving mechanisms, levee failures can be due to (a) geotechnical failures, (b) excessive amounts of water passing over the levee (i.e., hydraulic failures), or at the later stage, an initiation of a breach related to specific failure mechanisms (Sharp et al., 2013). For many failure mechanisms (Figure 1), deformation is an important early indicator for imminent failures (Dentz et al., 2006; Hanssen & van Leijen, 2008; Özer, van Damme, Schweckendiek, & Jonkman, 2016). Early detection of these indications would facilitate on-time levee assessment and maintenance before a failure occurs (Tarrant, Hambidge, Hollingsworth, Normandale, & Burdett, 2017). Therefore, improved methods to detect small deformations of levees at an early stage are likely to give a significant contribution to levee safety.

Conventional levee monitoring methods mainly consist of visual inspections (Cundill, van der Meijde, & Hack, 2014; Mériaux & Royet, 2007; Sharp et al., 2013), restricted to a typical frequency of twice a year in the Netherlands (Bakkenist, van Dam, van der Nat, Thijs, & de Vries, 2012). During these inspections, the integrity of the structures is assessed using qualitative inspection parameters (Bakkenist, 2012), for example, by checking the presence of any damage, crack, animal burrows, or irregular vegetation on the levees. Although some of these features may be clearly visible, many failure modes of levees are usually preceded by small and slow changes in geometry and structure, which may not be detectable by visual inspections (Tarrant et al., 2017). Remote sensing techniques are usually applied only for the locations at which a problematic situation has been detected by visual inspections (Bakkenist & Zomer, 2010; Moser & Zomer, 2006). Methods using advanced in-situ sensors instrumentation are also available (Cundill et al., 2014), but are difficult to deploy at the extended spatial scales involved with levee systems due to the costs and work load requirements. Consequently, current detection and monitoring methods are still strongly reliant on time-consuming evaluation of expert judgments, which may result in subjective, infrequent, and qualitative assessments (Bakkenist & Zomer, 2010; Hanssen & van Leijen, 2008; Rijkswaterstraat, 2001; Swart, 2007). Hence, especially in countries with extended flood defence infrastructure, such as the Netherlands, there is a need for innovative and cost-effective techniques to monitor levee conditions, that should be applicable on a wide scale with good precision and requiring less resources.

Over the last decades, satellite remote sensing techniques have evolved rapidly. Satellite radar interferometry, or Interferometric Synthetic Aperture Radar (InSAR), has become

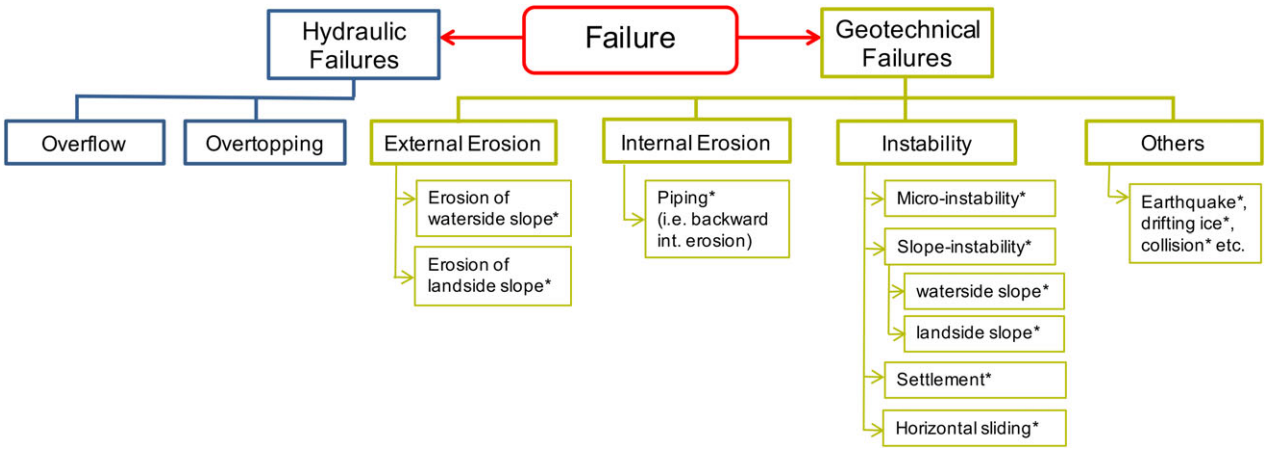

FIGURE 1 Overview of the most common flood defence failure mechanisms, see, for example, Sharp et al. (2013). Failures that have deformation as an (early) indicator are marked with asterisk (*)

an efficient tool to monitor the stability or deformation of the earth's surface (Hanssen, 2001; Stramondo et al., 2016). It instantaneously provides millions of observations with meter-level spatial resolution and millimetre-level precision, supported by revisit times in the order of days, at very low costs compared to conventional surveying methods. In particular, the Persistent Scatterer InSAR (PS-InSAR) methodology is routinely applied because of its ability to detect high-quality and consistent scattering points on the surface. The wide range of InSAR applications includes urban areas (Gernhardt, Adam, Eineder, & Bamler, 2010; Schunert & Soergel, 2012), railways (Chang, Dollevoet, & Hanssen, 2017), dams (Perissin & Wang, 2011), highways (Perissin, Wang, & Lin, 2012), and tectonic movements (Hooper, Segall, & Zebker, 2007). Especially in the Netherlands, InSAR has been successfully applied to monitor land deformation, for example, due to ground water extraction (van Leijen & Hanssen, 2008), peat soil decomposition (Cuenca & Hanssen, 2008), sinkhole detection (Chang & Hanssen, 2014), gas extraction (Hanssen et al., 2007; Ketelaar, van Leijen, Marinkovic, & Hanssen, 2006), and mining (Cuenca, Hooper, & Hanssen, 2013).

Monitoring levee systems using InSAR provides high precision in long-term deformation estimates compared to the conventional methods. Dentz et al. (2006) explore the technical feasibility of InSAR for levee deformation monitoring and suggest a collaboration of radar and levee experts to improve the application of the technique. Hanssen and van Leijen (2008) demonstrate that with such method, levee deformations can be effectively monitored. Dixon et al. (2006) focus on the application of InSAR for monitoring the subsidence of New Orleans, USA, concluding that the highest subsidence rates observed between 2002 and 2005 match with the levees of the Mississippi River–Gulf Outlet canal that breached catastrophically during Hurricane Katrina in 2005.

Here, we provide a comprehensive overview of the state of the art in using time-series InSAR for systematic levee deformation monitoring, aiming to assess its usability and applicability as a way of complementing existing monitoring approaches and failure investigation methods. A general review of the basic principles of InSAR and PS-InSAR is introduced. Its applicability on levee management, which is influenced by different factors such as vegetated surface cover, is discussed with the support of different case studies in the Netherlands. We clarify the most important technical aspects with respect to levee monitoring using InSAR technology, such as deformation estimation in different directions, satellite characteristics, precision, and reliability. Moreover, we discuss the potential of using satellite radar imaging for levee monitoring, and analyse the links between levee deformations and various failure mechanisms.

2 | METHODOLOGY

2.1 | Basic concepts of InSAR

Synthetic aperture radar (SAR) technology uses active radar sensors that transmit pulses of electromagnetic waves from space to Earth and record the back-scattered signals from the earth's surface. These signals are then used to construct an image, in which each resolution cell, or pixel, comprises the coherent sum of all reflections within that cell. This coherent sum has an amplitude, A, expressed in dB (i.e., the back-scatterer magnitude), and a phase, ψ, expressed in radians, which is stored as a complex number, named phasor, P, per pixel (Hanssen, 2001);

$$P = Ae^{i\psi} \tag{1}$$

where i is the imaginary number. The amplitude, A, is a function of the slope, distribution, roughness, and electrical properties of the objects in the resolution cell, as well as sensor characteristics, such as wavelength, λ, bandwidth, and incidence angle, θ_{inc}. The phase, ψ, is a function of the time delay between signal transmission and reception, but also influenced by the random distribution of all scatterers within the resolution cell.

The main principle of InSAR for deformation estimation is to interfere at least two SAR images acquired at different times over the same location (Bamler & Hartl, 1998; Hanssen, 2001), creating a so-called interferogram. Applied to levees, differences in amplitude between two images show the changes in reflection behaviour of the levee cover, whereas phase differences can be exploited to extract information about the displacements between two acquisition times, with millimetre-level precision (Figure 2).

The interferometric phase of a pixel, that is, the difference between the phase values acquired at different times, includes several (a) "coherent" components, such as earth curvature, topography, atmospheric delay, and surface displacement, and (b) "incoherent" components, due to changes in the scattering mechanisms at the earth's surface, for example, due to vegetation and measurement noise (Hanssen, 2001; Zebker & Villasenor, 1992). The aim of any InSAR technique is to isolate the coherent signal of interest, for example, the displacement phase, from the other phase contributions. In general, this isolation of the different coherent components is achieved by using time-series of tens to hundreds of acquisitions, which is possible for all pixels for which the incoherent components of the signal are not too dominant (Berardino, Fornaro, Lanari, & Sansosti, 2002; Colesanti, Ferretti, Novali, Prati, & Rocca, 2003; Ferretti, Prati, & Rocca, 2001).

2.2 | Time-series processing

The value of SAR imaging for levee monitoring is highest when time-series approaches are used. Current satellite constellations allow for near-daily acquisitions from varying viewing geometries, with different resolutions, and irrespective of

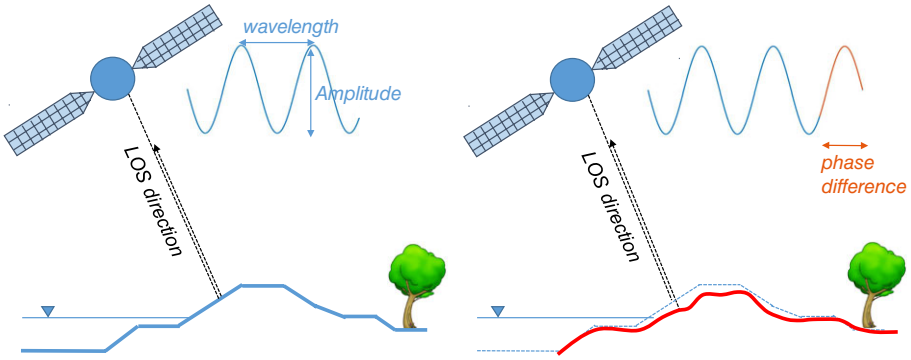

FIGURE 2 Two sequential Interferometric Synthetic Aperture Radar (InSAR) measurements before and after deformation occurs on a levee body. Displacement (mm) is measured in the line-of-sight (LOS) direction, that is, in the line between the satellite and the scatterer, as a fraction of the radar wavelength

cloud cover and solar illumination (Berger, Moreno, Johannessen, Levelt, & Hanssen, 2012). There is a wealth of information to be gained from the SAR pixel time-series (Figure 3). Amplitude variability holds information on surface roughness and soil moisture changes, while the full complex per-pixel information can be exploited in an interferometric sense for measuring displacements, referred to as deformations in the rest of the paper. Various time-series processing techniques may be applied to estimate the deformations from the data. PS-InSAR uses dominant point-like scatterers with a persistent scattering (PS) behaviour over time. This type of scatterers typically shows a coherent phase behaviour over long periods of time. Distributed scatterers (DS) exploits groups of pixels which have no dominant scatterers but have a similar phase behaviour over the group (Figure 3) (Crosetto, Monserrat, Cuevas-González, Devanthéry, & Crippa, 2016; Osmanoğlu, Sunar, Wdowinski, & Cabral-Cano, 2016).

The most suitable approach depends on the surface cover, the number of available radar images, the orientation of the structures and the expected deformation signal. In this study, we focused on the PS-InSAR method, which is typically composed of three main steps; (a) creating multiple interferometric combinations from complex data ("stack processing"), (b) detecting PS and estimating their deformation phase ("PSI analysis"), and (c) assessing the quality of the results. The interferometric stack processing of the radar data is performed using the Delft Object-oriented Radar Interferometric Software (DORIS) (Kampes, Hanssen, & Perski, 2003). These radar interferometric data stacks contain dozens of image acquisitions, each with billions of image pixels. The PSI analysis aims to detect those pixels with a coherent phase behaviour. The Delft implementation of Persistent Scatterer Interferometry (DePSI) (van Leijen, 2014) algorithm is applied to transform the radar data stack into a set of detected PS on the levee surface and their deformation time-series are estimated. Lastly, a quality assessment is performed using additional quality metrics to remove the incorrectly detected PS and to describe the quality of the final results. For a detailed description of the processing approach and a comparison of several PS-InSAR techniques, see Crosetto et al., 2016; Samiei-Esfahany, 2017; van Leijen, 2014.

3 | CHARACTERISTICS, APPLICABILITY, AND QUALITY

3.1 | Satellite characteristics

All available SAR satellites are in a so-called sun-synchronous polar orbit, moving both from south to north

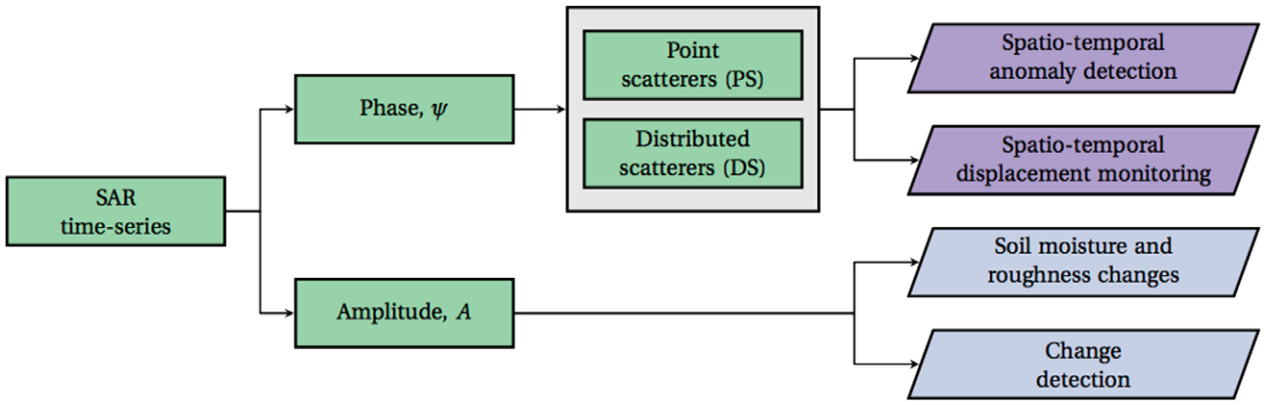

FIGURE 3 Overview of the Synthetic Aperture Radar (SAR) methods, observables, and physical parameters. The time-series of amplitude and phase can be used to derive several products for levee monitoring

(ascending) and from north to south (descending) (Figure 4). This allows satellites to monitor a particular area from at least two viewing directions. For higher altitudes, there are generally more orbits that cover the same area on the ground, leading to a higher revisit rate.

SAR satellites provide radar images from 1992 to the present to monitor surface motion. Thus, historical deformation, for which no other survey data may be available, can be investigated since satellite data are archived for further exploitation. An overview of the most important past and current radar satellite missions suitable for levee deformation monitoring is given in Table 1.

One of the attractive characteristics of the radar instruments in these orbits is the day and night monitoring of the earth's surface in all weather conditions, which provides frequent data acquisitions at low cost. Moreover, the wide areal coverage enables a global perspective on deformation behaviour using huge amounts of data from various satellites with high spatial and temporal resolution. Its high measurement accuracy allows us to monitor small deformations at mm-level, depending on the characteristics of the radar and the conditions of the monitored levee.

Technological developments and new generations of satellites and sensors led to significant improvements in SAR data with reduced repeat time or increased spatial resolution (Schunert & Soergel, 2012), see Table 1. To demonstrate the differences between sensors, Figure 5 shows the levees on the island of Marken, the Netherlands, using medium resolution satellites, ERS (1992–2000), Envisat (2003–2010), and a high-resolution satellite, TerraSAR-X (2009–2016). Figure 5a,b shows that the levees present deformation velocities for the two different time periods obtained from ERS and Envisat satellites. Figure 5c reveals that the higher spatial resolution results in a strong increase of the number of PS points compared to the results of ERS and Envisat. This can be explained by the fact that PS-InSAR detects one PS point per cell, and consequently a smaller resolution cell leads to more PS per km^2. Moreover, the measured deformation values and the absolute positions of the measurement points are estimated more precisely. Additionally, the reduced repeat cycle of a X-band satellite (11 days) allows for monitoring the levees more frequently. Note that all results show significant deformation rates on the north and south levees of the island.

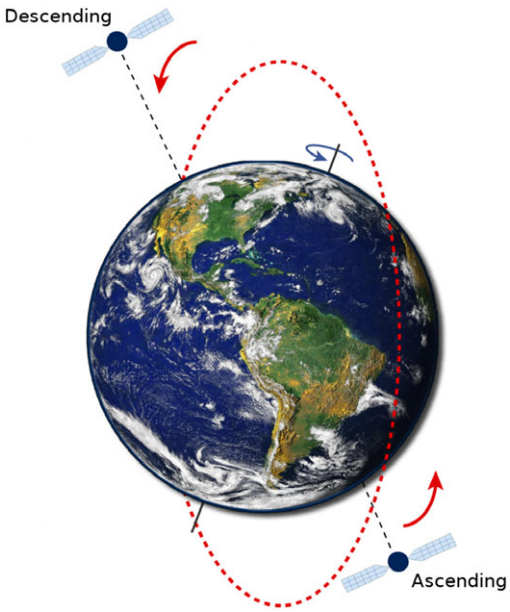

FIGURE 4 Satellite orbit, consisting of an ascending and a descending part (source: SkyGeo)

All deformation estimates obtained by PS-InSAR are projections of the three-dimensional (3D) deformation vector onto the line-of-sight (LOS) direction of the satellite. This direction from satellite to object is determined by the heading angle of the satellite with respect to the north, α_h and the incidence angle of the radar, θ_{inc}. In the figures in this study, which have North on top, the heading of the satellite is expressed by a vector accompanied by an orthogonal viewing direction of the satellite (top view). The incidence angle is here defined as the vertical angle relative to the plumb line (Figure 6).

3.2 | Observation characteristics

The usability and applicability of InSAR depends largely on the type of observations and their quality. In this section, we describe the characteristics of observations, their quality assessment, and precision.

3.2.1 | Observables

The SAR phase values per scatterer (observation point or PS point) and per acquisition are called *input observables*. From these we can obtain *derived observables*, such as the (a) the difference in phase between two acquisitions for one scatterer (i.e., change in time per location), (b) the difference in phase between two scatterers for one acquisition (i.e., change in space at a given time), and (c) the difference between (a) and (b). The latter is termed the double-difference phase observable, and it forms the basic element in interferometric analysis (Hanssen, 2004). In other words, the double-difference between two PS points on a levee is used to quantify the deformation occurring between two time instants at one location relative to the deformation at the same time instants at the other location.

3.2.2 | Relativity

Deformation time-series of PS in every data set are relative to each other: the double-difference observations. Integrating the differences to a common reference point and a reference time may be convenient in the visualisation, but is not strictly necessary. Thus, the radar measurements are inherently relative in time and space. When absolute motion estimates are desired, PS-InSAR measurements can be transformed into a common geodetic datum (Mahapatra, Samiei-Esfahany, van der Marel, & Hanssen, 2014).

TABLE 1 Most important past and current radar satellite missions suitable for levee deformation monitoring and their characteristics

Mission	Time period	ΔT_{rep} (days)	ΔT_{rev} (days)	Band	Spatial resolution (m)	Precision[b] (mm)	λ (mm)	θ (deg)	Availability
ERS-1/2	1991–2000[a]	35	8	C	4 × 20	1.4	56	23	Free
Envisat	2002–2010	35	8	C	4 × 20	1.4	56	23	Free
RadarSAT-2	2007–	24	6	C	10 × 9[c]	1.4	55	20–49	Commercial
TerraSAR-X/Tandem-X/Paz	2007–	11	3	X	3 × 3[c]	0.8	31	20–45	Commercial
Cosmo-Skymed 1/2/3/4	2007–	4	1	X	3 × 3[c]	0.8	31	20–60	Commercial
Sentinel-1a/b	2014–	6	2	C	20 × 5[c]	1.4	55	29–46	Free

Notes. ΔT_{rep}, orbital repeat cycle; ΔT_{rev}, potential revisit time for mid-latitudes; λ, radar wavelength; θ, incidence angle (ascending-descending).
[a] After 2000, ERS-1/2 was not suitable anymore for deformation applications.
[b] Equivalent precision of the phase measurement, assuming a signal-to-noise ratio of 10 dB (~5% of the semi-wavelength).
[c] Higher spatial resolutions are possible for specific instrument modes.

3.2.3 | Measurement precision

The measurement precision expresses the quality of the *input observables,* that is, the SAR phase values per scatterer. This precision is dependent on the thermal noise floor of the SAR instrument and on the amount of backscatter received from the earth. While the latter part is location-dependent, we typically work with scatterers with a signal-to-noise ratio (SNR) level of 10–24 dB, which translates to a precision of 5–1% of the semi-wavelength of the radar (see Table 1). Expressed in millimetres, this yields precisions (standard deviations) between 0.2 and 1.4 mm, which is why the technique is said to have mm-level precision.

The precision of the *derived observables* (the double-differences) follows from error propagation. If the input

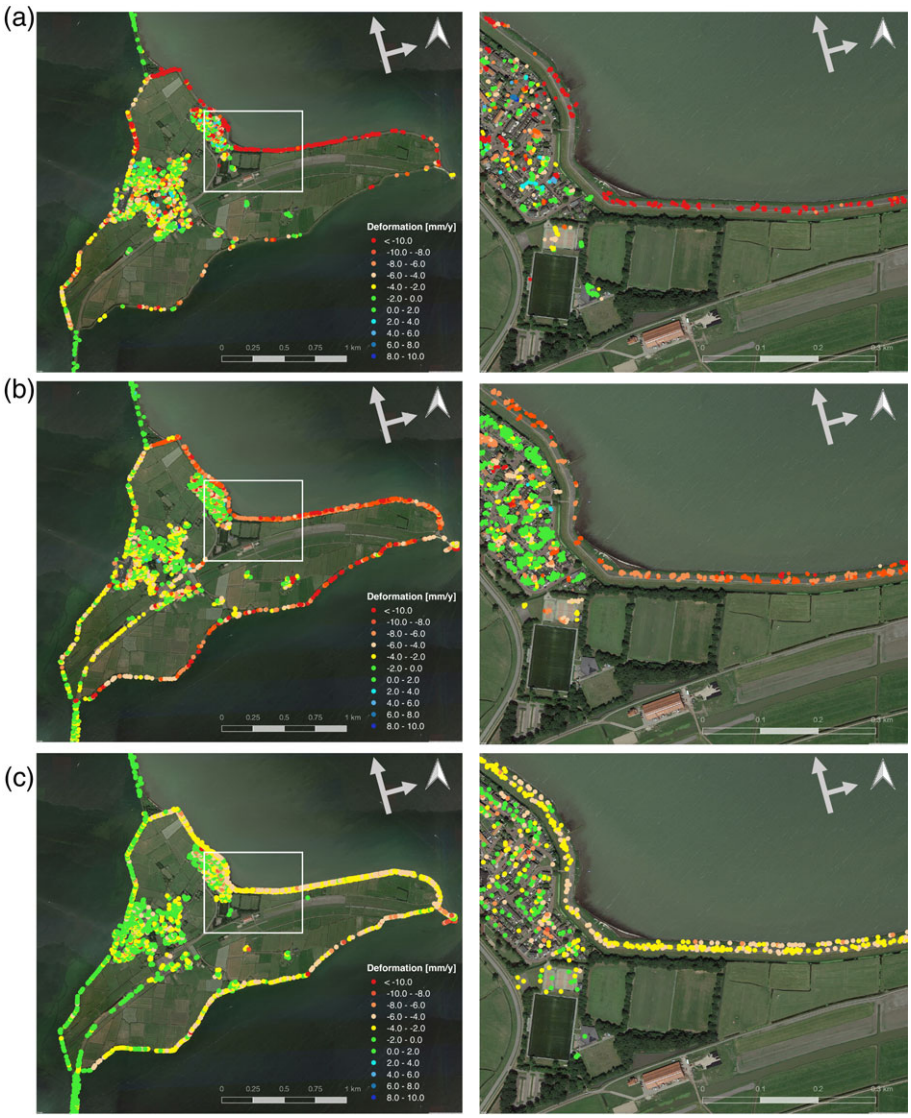

FIGURE 5 Relative deformation velocity maps of Marken monitored by (a) ERS (1992–2000), (b) Envisat (2003–2010), (c) TerraSAR-X (2009–2016)

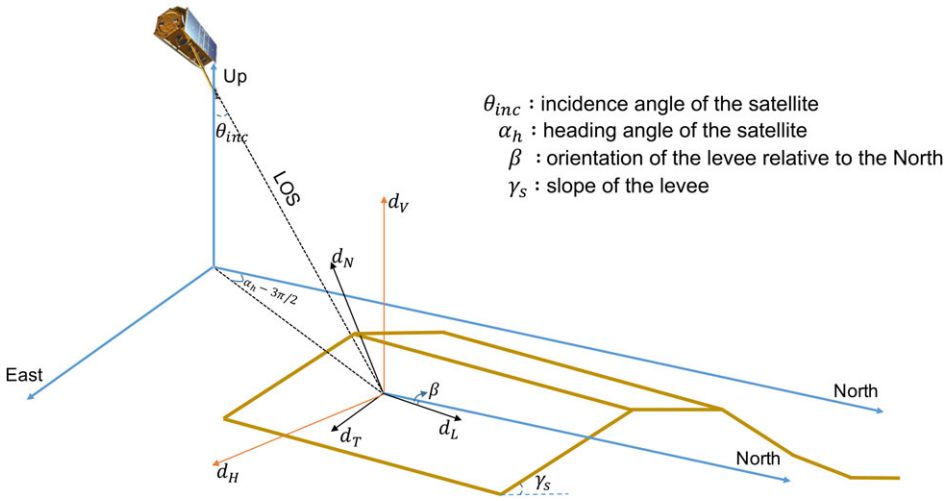

FIGURE 6 Three-dimensional coordinate transformations for levee section from the line-of-sight (LOS) vector to a local Cartesian reference system

observables are considered to be independent (uncorrelated), the precision of the double-differences would be doubled, that is, between 0.4 and 2.8 mm. However, these precisions are feasible only under the assumption that the observations for a single scatterer in two acquisitions are completely correlated or "coherent." In practice, however, this assumption may not be valid for a large number of pixels in an image. As a consequence, the measurement precision of the double-difference observations may be much lower, a process termed temporal decorrelation. Since the degree of temporal decorrelation is not related to the original measurement precision anymore, but rather to the conditions on the earth's surface, the precision of the double-difference observations turns out to be very variable spatially. In fact, the vast majority of scatterers is often "incoherent," and therefore not useful for retrieving geometry changes. Fortunately, there are billions of observations in a SAR image, and therefore the survival of a limited percentage does still yield very high point densities, as proved by the examples in the figures.

3.2.4 | Parameters

The double-difference phase measurements are the input for the parameter estimation. These phase measurements are sensitive to a number of unknown parameters, such as their topographic position, to the variable delay of the radio signal through the atmosphere, to the deformations, and are ambiguous, or "wrapped," to values between 0° and 360°. All these parameters need to be estimated from the phase measurements, which is the main challenge of the interferometric data processing. For levee monitoring, the deformations are the main parameters of interest, which can be further parameterized as a time-series of LOS deformations, or as parametric or non-parametric functions fitting the deformations. Expressed as a single relative velocity per point, these parameters can be easily visualised on a plane map projection.

3.2.5 | Quality assessment

The double-difference nature of the measurements yields double-difference deformation parameters. The quality of these parameters can be expressed by a variance–covariance matrix, which is generally a full matrix. Note that the non-zero covariance in the matrix causes the quality of the results to be independent of the choice of the location or time of the reference point. When a specific parametric model is chosen to describe the deformations over time, the residues between the observations and the model can be used as a posteriori quality metric, equivalent to a goodness-of-fit metric (van Leijen, 2014). Obviously, this metric does not only express noise or errors in the measurements, but the degree of applicability of the chosen temporal model as well.

3.2.6 | Geo-localization

In PS-InSAR processing, a precise geo-localization of PS points is necessary to interpret the results correctly. Positioning of the PS points is less precise than their deformation estimates. The positioning precision is 1–2 m for C-band data and less than 1 m for X-band data (Dheenathayalan, Cuenca, Hoogeboom, & Hanssen, 2017). Using the exact PS locations, reflections from the ground can be separated from those originating from higher level objects, which may show a different deformation behaviour (Dheenathayalan, Small, Schubert, & Hanssen, 2016). Georeferencing is thus of high importance in the analysis of the results, in particular when the deformation is localised (Chang & Hanssen, 2014).

3.3 | Applicability

While the radar satellite images cover the entire earth, not every pixel contains a valuable deformation measurement. As discussed above, the main condition for this applicability is the degree of coherence. The coherence, γ, is a number in the range [0,1] that expresses the degree to which radar pixels can be compared over time. A value of 1 relates to perfect comparability, while a value of 0 implies that the

radar signal is not comparable. The coherence of the PS depends on the consistency and electrical properties of the surface. Vegetation and its temporal dynamics and soil types have a direct influence on the coherence, and thus the availability of PS (Morishita & Hanssen, 2015b). Most of the coherent scatterers stem from non-vegetated areas, such as the waterside slope of the levee with rock revetments. To illustrate this, the mean coherence estimates per pixel were calculated for a levee segment at Marken that was examined in Figure 5. For this specific levee segment, the difference between water (low coherence) and the levee as a line structure can be clearly identified in Figure 7. Considering the radar look direction and the surface cover, the points with high coherence are mostly from the non-vegetated waterside slope of the levee, that is, the rubble at the toe, paths, and revetments near the crest.

The condition of coherence limits the spatial coverage over the levee profile, and therefore the applicability of the technique. However, for wider deformation signals, measured deformations from one area can be an indication of another part of the levee. Moreover, recent approaches on estimating deformation in areas with low coherence, and in the absence of sufficient PS appear to be promising (Morishita & Hanssen, 2015a, 2015b). A low PS density can also be overcome by installing in-situ devices, that is, corner reflectors or active transponders, which provide a strong signal in the SAR images resulting in adequate deformation estimates (Dheenathayalan et al., 2016; Mahapatra et al., 2014; Sarabandi & Chiu, 1996).

3.3.1 | Case studies

The applicability of levee deformation monitoring using the PS-InSAR approach is demonstrated via case studies located in different parts of the Netherlands. The long-term deformation behaviour of these levees has been estimated from both ascending and descending orbits, using available satellite acquisitions in order to estimate the deformation time-series of each PS point for different time periods. Although the processing results may generally be visualised by a constant (linear) deformation rate, every PS point has a complete time-series of deformation estimates in the LOS direction. Figure 8 shows the results of levee deformation monitoring in Zeeland, in the South-west of the Netherlands, using satellite images acquired by RadarSAT-2 from a descending orbit, between 2010 and 2017. In the same figure, an example for a deformation time-series of one of the PS points is shown. These time-series enable historical analyses over the observed period to have a better understanding of levee behaviour in time. Besides, they also have an importance for detecting anomalies, which could be further evaluated by the levee authorities. Indeed, locations marked in red in the figure represent deformations greater than 5 mm per year, which may be indicative of an anomalous levee behaviour. For these locations, additional field observations and analyses could be relevant to evaluate the causes of the behaviour and the effects on safety, for example, on the likelihood of overtopping resulting from subsidence.

Figure 9 shows the results from levee deformation monitoring in Flevoland, the Netherlands, which is an area reclaimed from the sea in the late 60s. Linear deformation rates for each coherent scatterer along the monitored levees have been estimated using Envisat from a descending orbit, during 2003–2010. What can be observed from the figure is a clear difference in the deformation rate of the different levee sections which, being close to each other, would be expected to have the same loading conditions and, thus, a similar behaviour. In this case, the largest deformation rates of the levee are found near the nature reserve Oostvaardersplassen where different water level management practices are applied than in the surrounding areas. Hence, this

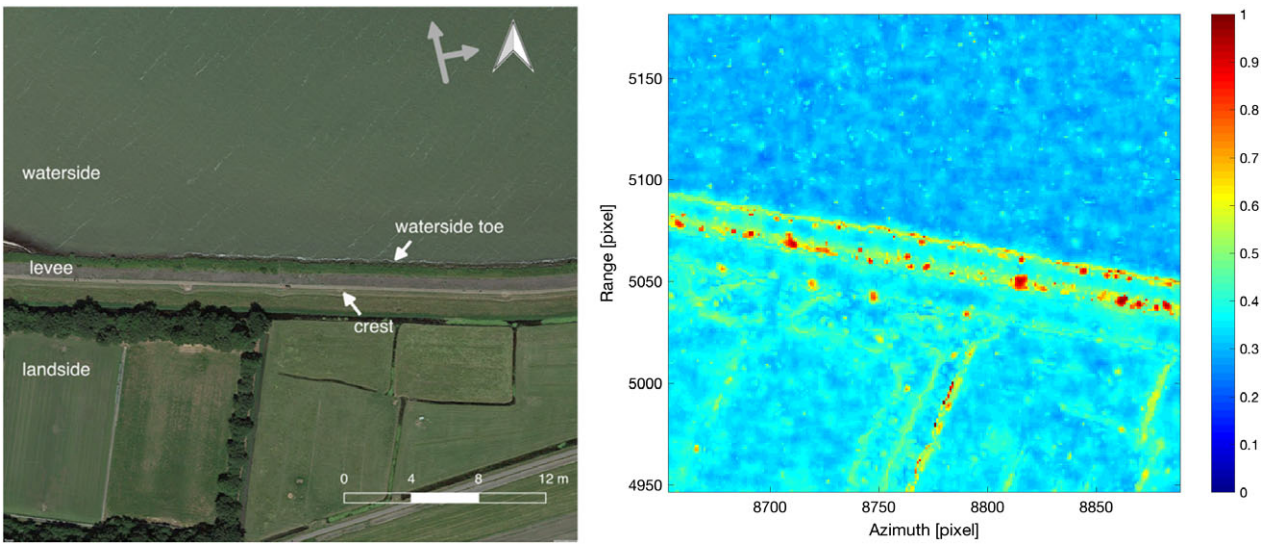

FIGURE 7 Left: Levee segment at the island of Marken, the Netherlands. Right: Coherence estimates of the pixels. Red colour represents high coherence, whereas blue colour shows the areas with low coherence. More information on coherence estimation and its bias is discussed by Hanssen (2001)

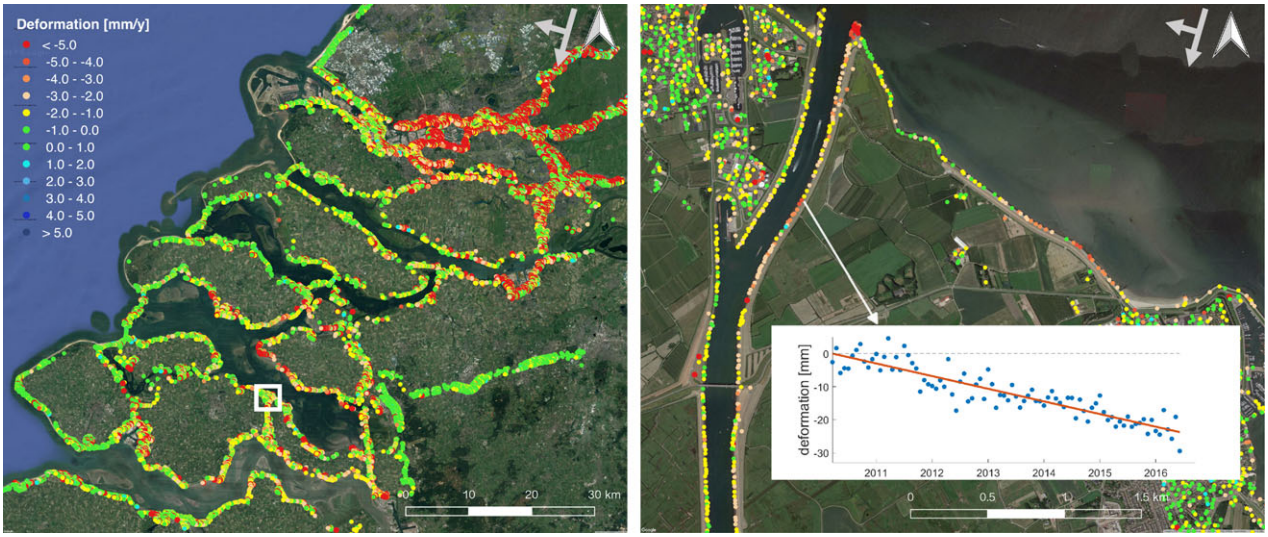

FIGURE 8 Left: Linear deformation rates (mm/year) of the levees in Zeeland, the Netherlands based on data acquired by RadarSAT-2, descending (2010–2017). Right: An example of deformation time-series with a linear velocity of 4.1 mm/year

example illustrates how the InSAR data, combined with other available information, such as loading conditions, soil characteristics, management, and maintenance, can support the levee assessments by identifying potential irregularities along the levees.

4 | PERFORMANCE ASSESSMENT

The previous section addressed the value of InSAR from a data-driven perspective, where the characteristics, applicability, and precision of the measurements were discussed. In the current section, we take a problem-driven perspective, focusing on the question whether it is possible to detect and monitor a specific type of levee deformation, such as a purely horizontal deformation, or a deformation parallel to the slope of a levee. As such, this is specific for a particular levee, and requires specific metrics, for instance, the particular detectability. This problem-driven approach is relevant for levee asset managers to determine whether it is feasible to detect a particular type of problem.

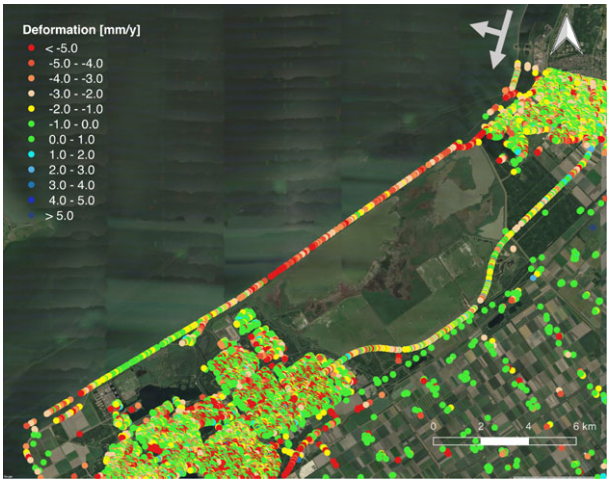

FIGURE 9 Linear deformation rates of a levee segment in Flevoland for the period of 2003–2010 using Envisat

4.1 | Sensitivity of deformation vectors

Deformations of levees occur in a three dimensional world, and can be expressed in a global or local reference system (Figure 6). Thus, the LOS observation from a radar satellite is a projection of the 3D deformation vector onto the LOS direction. Consequently, the observables in the LOS are sensitive to deformations in almost all directions, albeit with a varying degree of sensitivity. The degree of sensitivity, s, for different directions of the deformation vector varies between 0 ("no sensitivity"), and 1 ("maximum sensitivity"), and is defined as the projection length of a unit vector on the LOS direction (Chang, Dollevoet, & Hanssen, 2018). For line-infrastructure such as levee, we adopt a local reference system with a vertical axis, a longitudinal axis, and a horizontal complementing axis (Figure 6), where the direction of the longitudinal axis, in this case called the levee orientation, is determined relative to the North, with azimuth, β_a. Assuming that the deformation vector does not have a component in the longitudinal direction of the levee, we can express any deformation vector with a (β_a, ζ) coordinate pair, where ζ is the orthogonal elevation angle, in this case called the orientation of the deformation vector (Figure 10a). Here, $\zeta = 0^\circ$ corresponds to the horizontal direction to the land side, whereas $\zeta = 180^\circ$ is the horizontal direction at the water side. In Figure 10b, all possible deformation vectors are shown in the (β_a, ζ) plane, expressing the sensitivity values of a combined ascending and descending mission.

Figure 10b can be used to determine the particular observability of a specific deformation, based only on levee orientation and slope, even before satellite data is acquired. A sensitivity value higher than 0.3 typically implies that a

deformation is observable. Typical 1:2.5 levee slopes are indicated with the dashed lines. From this figure, it can be shown that generally all relevant levee deformations are observable within the levee profile.

Dividing the measurement precision (Table 1) by the product of the sensitivity, s, (Figure 10b), and the coherence, γ, yields a number that is proportional to the obtainable deformation precision (Hanssen, 2001). Subsequently, it is possible to devise metrics to determine the minimal detectable deformation (Chang et al., 2018), that is, how likely can a deformation of a given value be observed with a certain level of confidence, allowing levee asset managers to determine whether a particular deformation can be detected.

4.2 | Decomposition of deformation vectors

In the case when (a) radar images are available from two viewing directions, that is, ascending and descending orbits, (b) yielding measurements at the same geographic locations, (c) acquired in the same period of time, and (d) under the assumption that there is no longitudinal deformation (d_L=0), the actual direction of the deformation can be retrieved by combining two measurements in a vector decomposition (Ferretti et al., 2007) into normal (d_N) and transversal (d_T) directions or into vertical (d_V) and horizontal (d_H) directions (Chang, Dollevoet, & Hanssen, 2014).

Here, we analysed the sensitivity of horizontal deformation estimations for the primary flood defences in the Netherlands based on their orientations (Figure 11a). A purely horizontal deformation would be earlier detectable for the green segments that lay on the North–South direction with an orientation between −60°and +60°, whereas the orange and red segments, oriented in −90° to −75° and +75° to +90° range, would require a greater deformation to be detectable. Hence, the horizontal deformation of approximately 70% of the primary flood defences in the Netherlands can be retrieved with good accuracy (Figure 11b).

Although deformations in LOS direction can already give significant insight in levee deformations by providing binary spatial information on the stability of a levee (i.e., stable/unstable), two-dimensional (2D) deformation vectors can be particularly relevant for specific failure mechanisms. For instance, deformation in horizontal direction can be an early warning for an instability failure, for example, a peat levee failure near Wilnis, the Netherlands failed in the year 2005 due to a horizontal sliding (van Baars, 2005). Likewise, subsidence of the levee, which is mostly observed in vertical direction, would lead to hydraulic failures, that is, overtopping and overflow. In order to examine whether deformation vectors can be estimated from the SAR data, here we analyse a vector decomposition algorithm (Chang et al., 2014) that we adapted for levee conditions by using 142 ERS imagery acquired between 1992 and 2001. The method is demonstrated on a 75 km long levee along the Markermeer, the Netherlands, for which the deformation velocity maps from both ascending and descending orbits are given in Figure 12.

The deformation velocity (mm/year) with a relative standard deviation, σ, for each measurement point has been estimated from the deformation values by least-squares estimation over the time period considered. In the spatial domain, an interpolation is required since the observation locations for which ascending and descending images are available, are usually different. For the Markermeer levees, most of the reflections are from the waterside slope of the levee, which usually has some hard revetment. A distance-

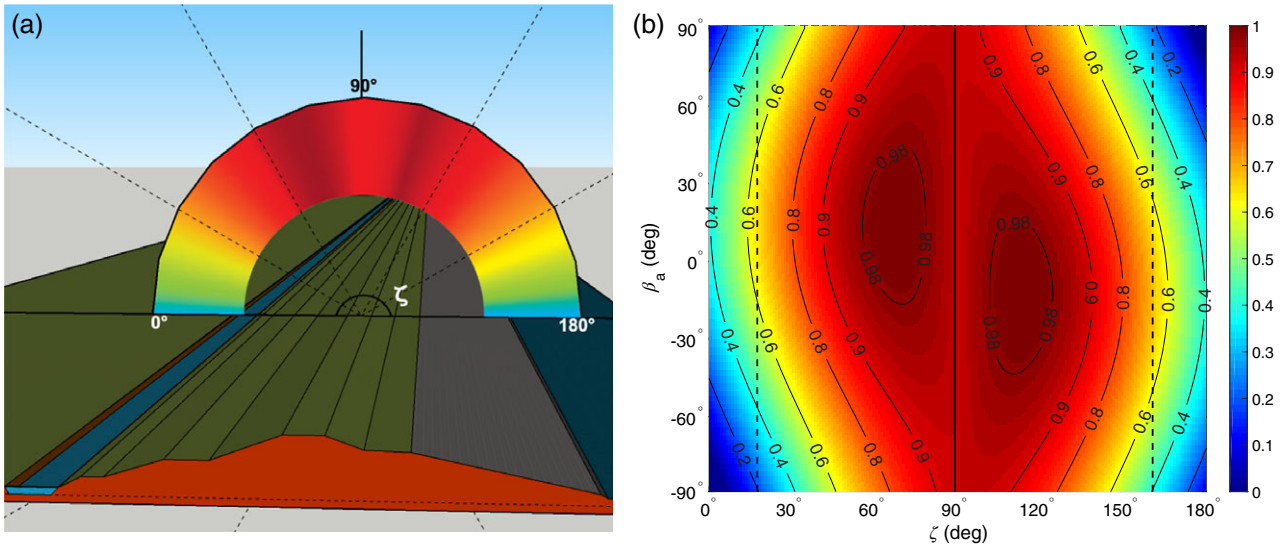

FIGURE 10 (a) Three-dimensional perspective orientation of a conceptual levee. Assuming no deformation along the longitudinal direction, any possible deformation direction is defined by (a) the orientation, β_a of the levee (here $\beta_a = 30°$), and (b) the orientation of the deformation vector, ζ, which runs from 0° to 180°. (b) Sensitivity direction plot, based on β_a and ζ, for a combined ascending/descending satellite viewing direction, expressing the sensitivity, s, of the measurements as a number between 0 and 1. The dashed lines indicate typical levee slope of 1:2.5, and the solid line indicates vertical deformations

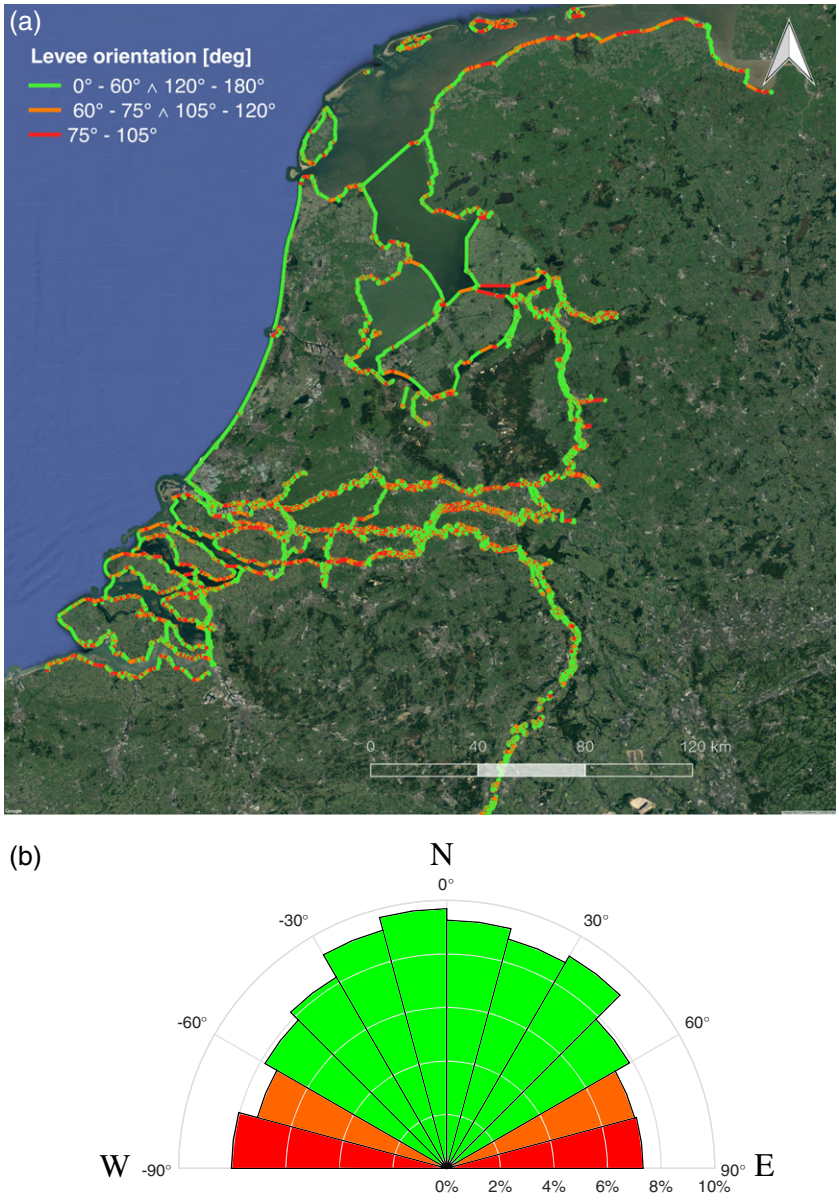

FIGURE 11 (a) Orientation of the primary flood defences in the Netherlands. (b) Polar histogram indicating the length (in percentage) of primary flood defences as a function of their orientation, with colours indicating the sensitivity to horizontal deformation

based interpolation method (inverse-squared distance weighting) (Fotheringham, Brunsdon, & Charlton, 2000) is used to interpolate an ascending deformation value on the location of the descending PS from close-by ascending PS's, assuming homogeneous characteristics. Considering the radar characteristics and the orientation and an average slope (1:2.5) of the levees, deformation velocity maps are decomposed into the four different directions (Figure 13). Related to the previous section on the sensitivity, values for the levee orientations outside the range of [−60°, +60°] have been removed based on their low SNR level.

To obtain a general idea regarding the estimation sensitivity of deformation velocities in (mm/year), the LOS standard deviations, σ, are propagated for each point. An analysis of the sensitivity of the linear deformation velocities shows that when the levee orientation is close to the E–W direction, the σ of the horizontal or transversal deformations increases. In Figure 14, standard deviations of the linear deformation velocities in transversal and normal directions are lower than 0.8 and 0.4 mm/year in the [−60°, +60°] range, respectively. Compared to transversal and normal directions, the sensitivity in the vertical direction is higher, with values of the σ of the linear deformation velocities lower than 0.2 mm/year, while the precision in the horizontal direction is lower than 1 mm/year, for the reasons discussed in the previous sections. This also reflects the larger variability for the horizontal estimates in Figure 13. In summary, it shows that levee orientation has an important effect on the observability of certain deformation components.

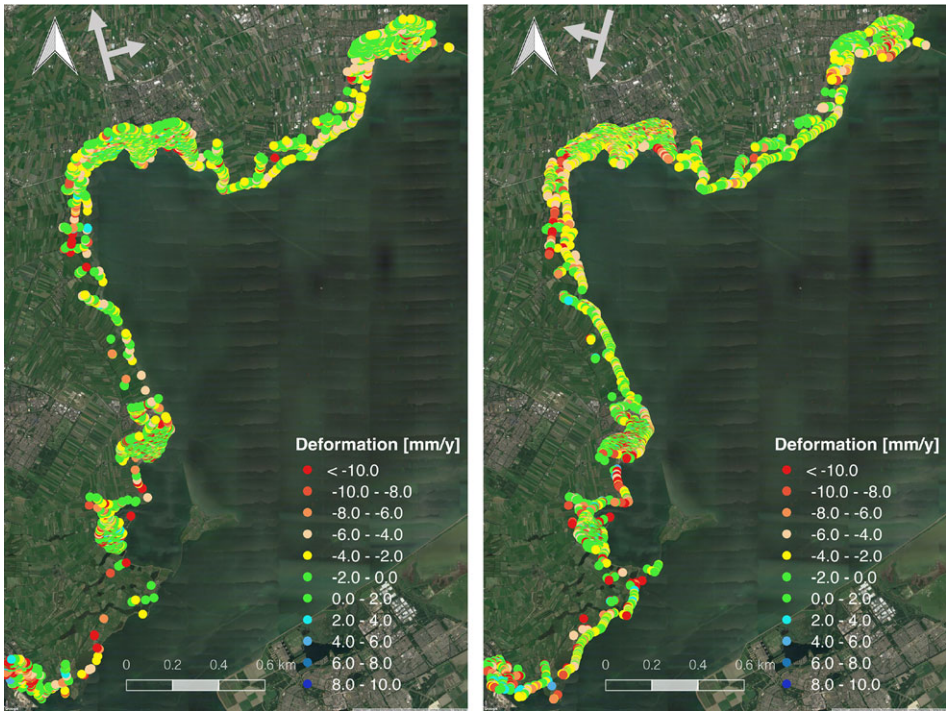

FIGURE 12 Linear deformation velocities (mm/year) in the line-of-sight (LOS) direction of the satellite for the Markermeer levee using the ERS satellite for the period of 1992–2001. Left: Ascending, right: Descending

5 | DISCUSSION ON THE POTENTIAL OF USING SATELLITES FOR LEVEE MONITORING

Although deformation of a levee can be classified in different ways, our final aim is to examine the observation of three main phenomena on different time scales (Figure 15). First, the long-term deformation behaviour of levees, progressing over years, can be monitored based on satellite and levee characteristics, for example, for processes such as subsidence. Second, the dynamic behaviour of levees can be due to varying loading conditions, such as the swelling and shrinkage behaviour related to changing water levels, temperature, or precipitation with seasonal and sub-seasonal changes, down to days. Third, levees can be subject to instantaneous deformations, such as irregularities or sudden changes in the deformation time-series. This includes a sudden failure when the load on the levee exceeds its strength, usually in a time scale of hours to days. Identifying if and when such a failure may suddenly happen is a crucial question with respect to safety.

Being able to monitor the failure processes could contribute to the reduction of model uncertainties and to improvements in levee assessments. The temporal sampling of contemporary satellites allows us to monitor changes on a daily scale (e.g., Sentinel-1a, 6 days repeat cycle, average of 1–2 days revisit time in the Netherlands). Given this temporal sampling, geotechnical failures occurring in a range of hours to days may not be detectable (Figure 16). However, before any sign of a geotechnical failure becomes visible, the levee may have shown subtle degrees of deformations which could indicate a failure being imminent. The ability of detecting these anomalous behaviours, which may happen within a longer time span (from days to months) and can be interpreted as indicators of potential weak spots, is thus an important contribution to levee safety assessment (Figure 16). For example, before a piping failure occurs, the levee may have shown a certain degree of deformation (e.g., uplift) having a time span long enough to be detected. Likewise, anomaly indications of slope instability may be observed during rising water levels prior to the actual failure event as vertical deformations on the crest and larger horizontal deformations at the toe. Furthermore, seasonal changes in meteorological conditions, for example, long drought periods and the consequent shrinkage of the levee, can cause horizontal sliding, which may give anomaly indications (weeks to months) before the actual geotechnical failure occurs (hours to days).

In this context, it is most beneficial to detect (a) which location may be most prone to sudden failures and (b) which levee segments can be considered to be stable. Current satellite missions, having given spatial and temporal resolutions (indicated by means of the dashed lines in Figure 16), are capable of detecting these anomaly indications under certain conditions. A possible future application of SAR is the detection of deformation anomalies in the framework of an early warning system. This can be done by analysing the response of a levee under normal loading conditions in order to identify those locations at risk of failing during extreme loading conditions. Substantial deformations in normal

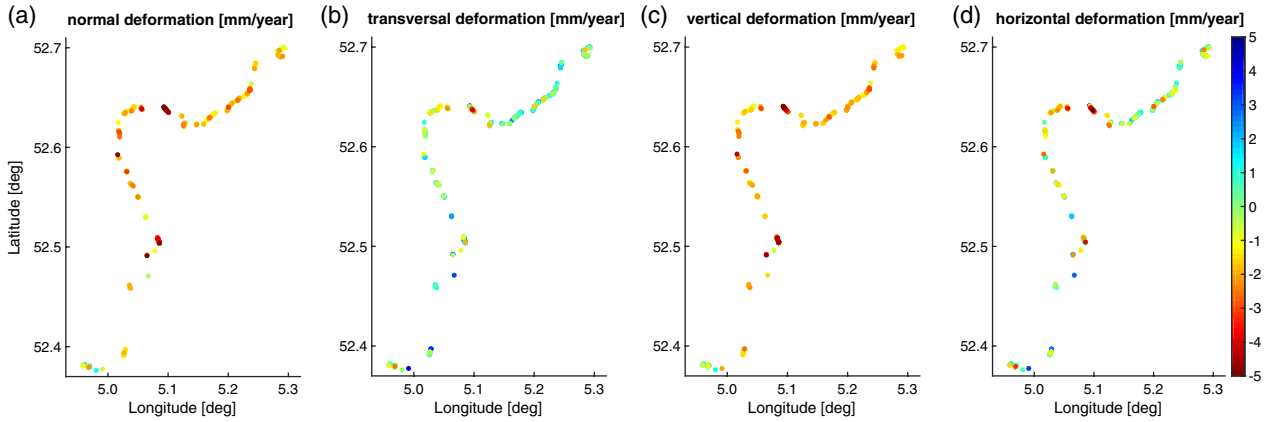

FIGURE 13 Deformation velocity maps (mm/year) decomposed in different directions: (a) normal d_N (b) transversal d_T (c) vertical d_V, and (d) horizontal deformations d_H for Markermeer levee monitored by the ERS satellite for the period of 1992–2001

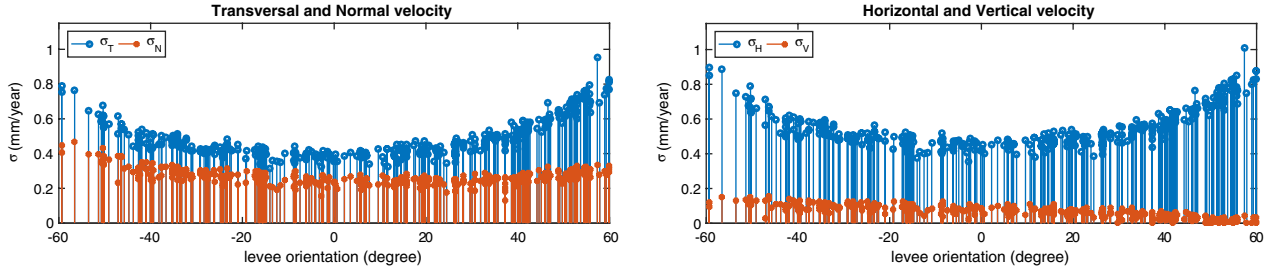

FIGURE 14 Standard deviations (mm/year) for the estimation of the decomposition vectors with respect to the levee orientations

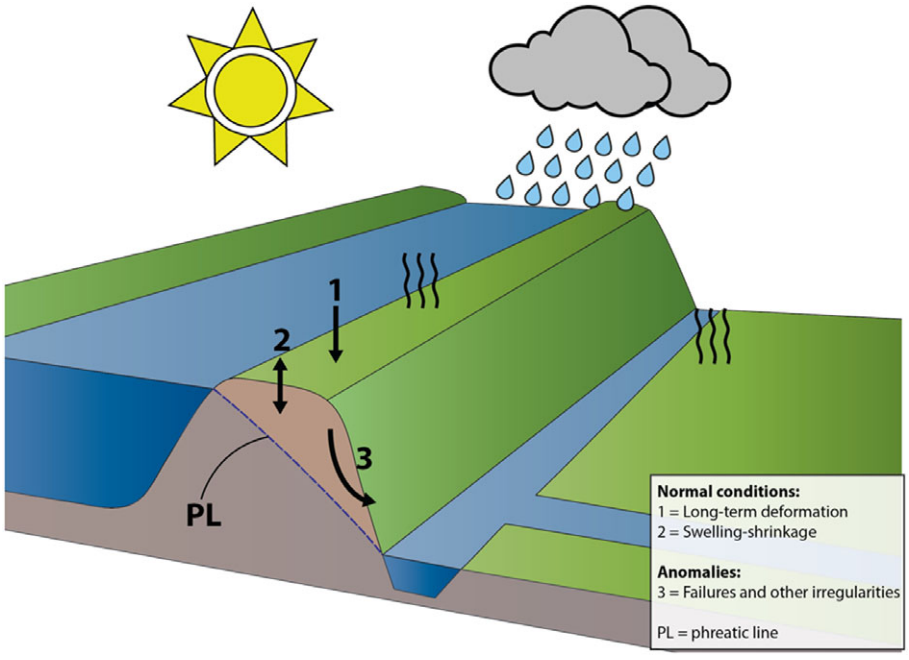

FIGURE 15 Three main phenomena on the levee behaviour

conditions could be precursors of a failure during more extreme circumstances. Even though two subsequent radar images are sufficient to create an interferogram, a longer time period (days to weeks, based on the precision of the observations and the satellite characteristics) may be required to be able to reliably detect an anomaly. Time-series analysis methods, for example, hypothesis testing (Chang & Hanssen, 2016) or machine learning techniques (van de Kerkhof, Pankratius, Chang, van Swol, & Hanssen, 2017) could be used to automate the assessment. Moreover,

as temporal and spatial resolution of satellite observations is expected to increase further, it may become possible in the future to observe geotechnical failures directly.

The potential of using SAR data can be explained by considering both the problem-driven and data-driven approaches. Operational management practice is generally considered as problem-driven in case of geodetic measurements. It is first decided what should be measured by levee managers, followed by hiring a contractor that can perform this task efficiently. Consequently, managers usually acquire what type of information they request with a uniform quality. However, InSAR provides data-driven information, which is not common in management practices. Observations highly depend on the satellite characteristics and local conditions. Hence, satellite observations may not be optimally matched to every specific case, in contrast to conventional in-situ techniques.

The relevant question in this respect is whether it is beneficial to use the information that is already available, even if there is no one explicitly requesting the data. Thus, InSAR data must therefore be seen as complementary to the conventional techniques, as "another tool in the toolbox." Especially countries having a strong expertise base and a full national InSAR coverage, such as the Netherlands, could improve their monitoring capabilities by making use of the frequent, abundant, and precise measurement data at a relatively low cost. Combining satellite data with other data sources (e.g., remote sensing and geological maps) and management information would provide a richer insight into understanding of levee behaviour. In the case of the 22,500 km of flood defences in the Netherlands, deformation data can be derived quantitatively on a daily basis which can complement levee management efficiently. Local in-situ measurements can be deployed effectively at those locations where it is needed. Also, additional geotechnical site analyses and safety assessments with models can be performed to get more information on the locations for which abnormal behaviours have been observed.

6 | CONCLUSIONS

Satellite radar imaging can be used to monitor the behaviour of levees, which allows to detect deformations on a daily scale with mm-level precision in all weather conditions at low cost. It provides historical deformation data (from 1992 to today), which can be used to investigate trends in deformation and to get more insight into levee behaviour mechanisms. Moreover, technological advances and new generation satellites led to significant improvements in SAR data with reduced revisit time (near-daily) and increased spatial resolution (e.g., 3 × 3 m), providing frequent observations with large areal coverage (km's).

Frequently recurring technical questions on levee monitoring using SAR technology, related to applicability, precision, and reliability were addressed. Various time-series processing techniques may be applied to estimate the deformations from the data. The most suitable approach depends on the surface cover, the number of available radar images, the orientation of the structures and the expected deformation signal.

The original *precision* of phase measurement of available satellites varies between 0.4 and 2.8 mm. However, the precision of the estimated observations is affected by the characteristics of the earth's surface (e.g., vegetation, soil

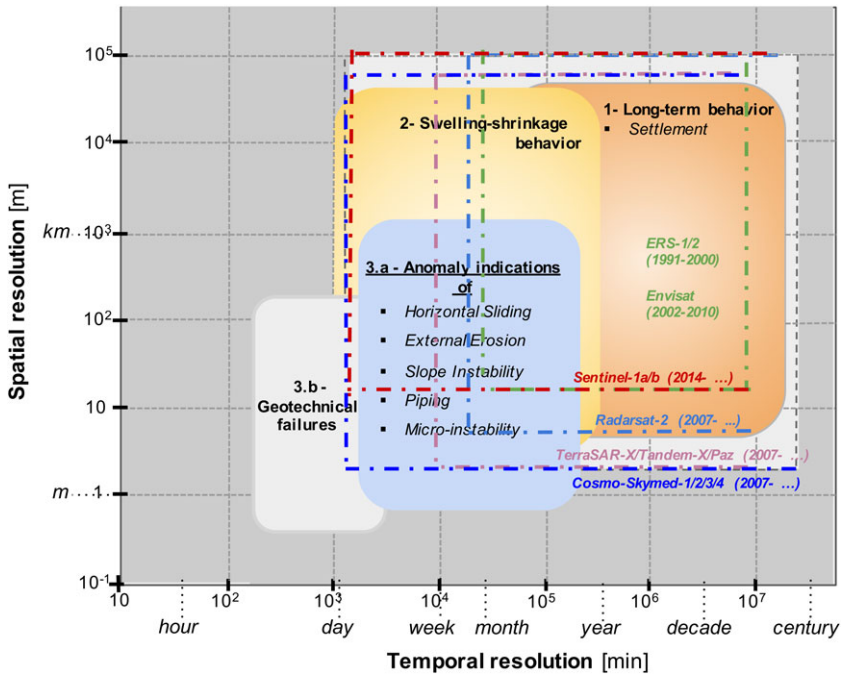

FIGURE 16 Log–log sensitivity diagram for the relation between levee behaviour and the satellite technology. Blue boxes represent the anomaly indications of the given geotechnical failure mechanisms. The numbers in the title of the boxes refer to the three main phenomena indicated in Figure 15

types), which determines the *coherence*, and by the orientation of the levee in combination with the deformation vector of interest, which determines the *sensitivity*. Hence, the actual precision of observation varies based on the area of interest. Although most of the coherent scatterers are generally obtained from non-vegetated areas (e.g., roads, revetments, etc.), they may provide an indication of the deformation behaviour of the rest of the levee. Thus, developing processing techniques to extract coherent signals from vegetated levees is an important research priority, with recent studies showing promising results. This would also extend the applicability to fully vegetated levees.

Through a number of examples in the Netherlands, we examined how satellite technology can be used to complement existing levee stability assessments. These cases also show that we can estimate any deformation vectors in almost all directions with varying degree of sensitivity depending on the orientation and the slope of the levee. A sensitivity plot is presented to conveniently assess the detectability of any kind of deformation. As an example, we showed that horizontal deformation for 70% of the primary flood defences in the Netherlands can be retrieved with high precision. Even though examples are shown only for the Netherlands, the applicability of this technology could be extended to other parts of the world, supporting levee management especially in countries with extensive flood defence infrastructures.

Although real-time monitoring of potential geotechnical failures is not possible given the temporal sampling of current satellites, sampling intervals (days) are two orders of magnitude higher than conventional monitoring (years). Given the increased temporal resolution, future research will focus on gaining a better understanding of levee behaviour, also in relation to loading conditions, and on detecting anomalies at an early stage, which can give indications of a levee failure being imminent. In summary, the deformation time-series can be used as (a) binary spatial information (i.e., stable/unstable), but also (b) for investigating the temporal behaviour of levee structures, and (c) to provide early warnings for anomalous behaviour preceding potential failures. We conclude that InSAR is moving from being a mere scientific tool towards an operational levee deformation monitoring system, with increased efficiency and quality. Consequently, the continuous analysis of InSAR levee deformation monitoring will assist the responsible levee authorities to take appropriate actions, hence avoiding catastrophic events and contributing to the flood risk reduction activities.

ACKNOWLEDGEMENTS

This research was performed as part of the NWO TTW project SAFElevee (project:13861). The authors would like to thank the German Aerospace Centre (DLR) for providing the TerraSAR-X data; the European Space Agency (ESA) for providing the ERS, Envisat and Sentinel-1 data; and the Netherlands Space Office (NSO) for making the RadarSAT-2 data available.

CONFLICTS OF INTEREST

The authors declare no conflicts of interest.

ORCID

Işıl E. Özer https://orcid.org/0000-0002-2022-1148

REFERENCES

Bakkenist, S. (2012). *Inspectiewijzers waterkeringen: technische informatie uitvoering inspecties*. Amersfoort, the Netherlands: STOWA (in Dutch).

Bakkenist, S., van Dam, O., van der Nat, A., Thijs, F., & de Vries, W. (2012). *Standaard inspectieplan: invulversie voor inspectieplan op maat*. Amersfoort, the Netherlands: STOWA (in Dutch).

Bakkenist, S., & Zomer, W. S. (2010). *Inspectie van waterkeringen: een overzicht van meettechnieken*. Amersfoort, the Netherlands: STOWA (in Dutch).

Bamler, R., & Hartl, P. (1998). Synthetic aperture radar interferometry. *Inverse Problems*, *14*(4), R1–R54.

Berardino, P., Fornaro, G., Lanari, R., & Sansosti, E. (2002). A new algorithm for surface deformation monitoring based on small baseline differential SAR interferograms. *IEEE Transactions on Geoscience and Remote Sensing*, *40*(11), 2375–2383.

Berger, M., Moreno, J., Johannessen, J. A., Levelt, P. F., & Hanssen, R. F. (2012). ESA's sentinel missions in support of earth system science. *Remote Sensing of Environment*, *120*, 84–90.

Chang, L., Dollevoet, R. P. B. J., & Hanssen, R. F. (2014). Railway infrastructure monitoring using satellite radar data. *The International Journal of Railway Technology*, *3*(2), 79–91.

Chang, L., Dollevoet, R. P. B. J., & Hanssen, R. F. (2017). Nationwide railway monitoring using satellite SAR interferometry. *IEEE Journal of Selected Topics in Applied Earth Observations and Remote Sensing*, *10*(2), 596–604.

Chang, L., Dollevoet, R. P. B. J., & Hanssen, R. F. (2018). Monitoring line-infrastructure with multisensor SAR interferometry: Products and performance assessment metrics. *IEEE Journal of Selected Topics in Applied Earth Observations and Remote Sensing*, *11*(5), 1593–1605.

Chang, L., & Hanssen, R. F. (2014). Detection of cavity migration and sinkhole risk using radar interferometric time series. *Remote Sensing of Environment*, *147*, 56–64.

Chang, L., & Hanssen, R. F. (2016). A probabilistic approach for InSAR time-series postprocessing. *IEEE Transactions on Geoscience and Remote Sensing*, *54*, 421–430.

Colesanti, C., Ferretti, A., Novali, F., Prati, C., & Rocca, F. (2003). SAR monitoring of progressive and seasonal ground deformation using the permanent scatterers technique. *IEEE Transactions on Geoscience and Remote Sensing*, *41*(7), 1685–1701.

Crosetto, M., Monserrat, O., Cuevas-González, M., Devanthéry, N., & Crippa, B. (2016). Persistent scatterer interferometry: A review. *ISPRS Journal of Photogrammetry and Remote Sensing*, *115*, 78–89.

Cuenca, M. C., & Hanssen, R. F. (2008). *Subsidence due to peat decomposition in the Netherlands, kinematic observations from radar interferometry*. Frascati, Italy: FRINGE2007.

Cuenca, M. C., Hooper, A. J., & Hanssen, R. F. (2013). Surface deformation induced by water influx in the abandoned coal mines in Limburg, The Netherlands observed by satellite radar interferometry. *Journal of Applied Geophysics*, *88*, 1–11.

Cundill, S. L., van der Meijde, M., & Hack, H. R. G. K. (2014). Investigation of remote sensing for potential use in dike inspection. *IEEE Journal of Selected Topics in Applied Earth Observations and Remote Sensing*, *7*(2), 733–746.

Dentz, F., Halderen, L., Possel, B., Esfahany, S. S., Slobbe, C., & Wortel, T. (2006). *Poseidon: On the potential of satelite radar interferometry for monitoring dikes of the Netherlands*. Delft, the Netherlands: Delft University of Technology.

Dheenathayalan, P., Cuenca, M. C., Hoogeboom, P., & Hanssen, R. F. (2017). Small reflectors for ground motion monitoring with InSAR. *IEEE Transactions on Geoscience and Remote Sensing*, *55*(12), 6703–6712.

Dheenathayalan, P., Small, D., Schubert, A., & Hanssen, R. F. (2016). High-precision positioning of radar scatterers. *Journal of Geodesy*, *90*(5), 403–422.

Dixon, T. H., Amelung, F., Ferretti, A., Novali, F., Rocca, F., Dokka, R., … Whitman, D. (2006). Space geodesy: Subsidence and flooding in New Orleans. *Nature*, *441*(7093), 587–588.

European Environment Agency. (2018). *European past floods [Online]*. Copenhagen, Denmark: Author. Retrieved from https://www.eea.europa.eu/data-and-maps/data/european-past-floods/

Ferretti, A., Prati, C., & Rocca, F. (2001). Permanent scatterers in SAR interferometry. *IEEE Transactions on Geoscience and Remote Sensing*, *39*(1), 8–20.

Ferretti, A., Savio, G., Barzaghi, R., Borghi, A., Musazzi, S., Novali, F., … Rocca, F. (2007). Submillimeter accuracy of InSAR time series: Experimental validation. *IEEE Transactions on Geoscience and Remote Sensing*, *45*(5), 1142–1153.

Fotheringham, A. S., Brunsdon, C., & Charlton, M. (2000). *Quantitative geography: Perspectives on spatial data analysis*. London, UK: Sage.

Gernhardt, S., Adam, N., Eineder, M., & Bamler, R. (2010). Potential of very high resolution SAR for persistent scatterer interferometry in urban areas. *Annals of GIS*, *16*(2), 103–111.

Hanssen, R. F. (2001). *Radar interferometry: Data interpretation and error analysis*. Dordrecht, the Netherlands: Springer Science+Business Media.

Hanssen, R. F. (2004). *Stochastic modeling of time series radar interferometry*. Geoscience and Remote Sensing Symposium. Anchorage, AK: IGARSS'04.

Hanssen, R. F. & van Leijen, F. J. (2008). *Monitoring water defense structures using radar interferometry.* Rome, Italy: IEEE. Radar Conference.

Hanssen, R. F., van Leijen, F. J., van Zwieten, G. J., Dortland, S., Bremmer, C. N., & Kleuskens, M. (2007). *Validation of PSI results of Alkmaar and Amsterdam within the Terrafirma validation project*. Frascati, Italy: FRINGE2007.

Heyer, T. (2016). Reliability assessment of levees based on failure investigations. *Vodohospodářské technicko-ekonomické informace*, *58*(3), 28–33.

Hooper, A., Segall, P., & Zebker, H. (2007). Persistent scatterer interferometric synthetic aperture radar for crustal deformation analysis, with application to Volcan Alcedo, Galapagos. *Journal of Geophysical Research – Solid Earth*, *112*, B07407.

Horlacher, H. B., Bielagk, U., & Heyer, T. (2005). Analyse der Deichbrüche an der Elbe und Mulde während des Hochwassers 2002 im Bereich Sachsen. Tech. Report 2005/09, Institut für Wasserbau und Technische Hydromechanik, Technische Universität Dresden, Dresden, Germany (in German).

Jorissen, R., Kraaij, E., & Tromp, E. (2016). *Dutch flood protection policy and measures based on risk assessment*. Lyon, France: FLOODrisk2016.

Kampes, B. M., Hanssen, R. F., & Perski, Z. (2003). *Radar interferometry with public domain tools*. Frascati, Italy: FRINGE2003.

Ketelaar, G., van Leijen, F., Marinkovic, P., & Hanssen, R. (2006). *On the use of point target characteristics in the estimation of low subsidence rates due to gas extraction in Groningen, the Netherlands*. Frascati, Italy: FRINGE2005.

Mahapatra, P. S., Samiei-Esfahany, S., van der Marel, H., & Hanssen, R. F. (2014). On the use of transponders as coherent radar targets for SAR interferometry. *IEEE Transactions on Geoscience and Remote Sensing*, *52*(3), 1869–1878.

Mériaux, P., & Royet, P. (2007). *Surveillance, maintenance and diagnosis of flood protection dikes: A practical handbook for owners and operators*. Versailles Cedex, France: Editions Quae.

Morishita, Y., & Hanssen, R. F. (2015a). Deformation parameter estimation in low coherence areas using a multisatellite InSAR approach. *IEEE Transactions on Geoscience and Remote Sensing*, *53*(8), 4275–4283.

Morishita, Y., & Hanssen, R. F. (2015b). Temporal decorrelation in L-, C-, and X-band satellite radar interferometry for pasture on drained peat soils. *IEEE Transactions on Geoscience and Remote Sensing*, *53*(2), 1096–1104.

Moser, G. M., & Zomer, W. S. (2006). *Inspectie van waterkeringen: een overzicht van meettechnieken*. Amersfoort, the Netherlands: STOWA (in Dutch).

Osmanoğlu, B., Sunar, F., Wdowinski, S., & Cabral-Cano, E. (2016). Time series analysis of InSAR data: Methods and trends. *ISPRS Journal of Photogrammetry and Remote Sensing*, *115*, 90–102.

Özer, I. E., van Damme, M., Schweckendiek, T., & Jonkman, S. N. (2016). *On the importance of analyzing flood defense failures*. Lyon, France: FLOODrisk2016.

Perissin, D., & Wang, T. (2011). Time-series InSAR applications over urban areas in China. *IEEE Journal of Selected Topics in Applied Earth Observations and Remote Sensing*, *4*(1), 92–100.

Perissin, D., Wang, Z., & Lin, H. (2012). Shanghai subway tunnels and highways monitoring through Cosmo-SkyMed persistent scatterers. *ISPRS Journal of Photogrammetry and Remote Sensing*, *73*, 58–67.

Rijkswaterstraat. (2001). *Hydraulische randvoorwaarden 2001 voor het toetsen van primaire waterkeringen*. Delft, the Netherlands: Rijkswaterstraat, DWW (in Dutch).

Samiei-Esfahany, S. (2017). *Exploitation of distributed scatterers in synthetic aperture radar interferometry.* (PhD thesis). Delft, the Netherlands: Delft University of Technology.

Sarabandi, K., & Chiu, T. C. (1996). Optimum corner reflectors for calibration of imaging radars. *IEEE Transactions on Antennas and Propagation*, *44*(10), 1348–1361.

Schunert, A., & Soergel, U. (2012). Grouping of persistent scatterers in high-resolution SAR data of urban scenes. *ISPRS Journal of Photogrammetry and Remote Sensing*, *73*, 80–88.

Schweckendiek, T., Vrouwenvelder, A. C. W. M., & Calle, E. O. F. (2014). Updating piping reliability with field performance observations. *Structural Safety*, *47*, 13–23.

Sharp, M., Wallis, M., Deniaud, F., Hersch-Burdick, R., Tourment, R., Matheu, E., … Durand, E. (2013). *The international levee handbook*. London, England: CIRIA.

Simm, J., Flikweert, J., Hollingsworth, C. & Tarrant, O. (2017). *Ten years of lessons learned from English levee performance during severe flood events.* 5th Annual Meeting of International Comminssion on Large Dams. Prague, Czech Republic: ICOLD.

Stramondo, S., Trasatti, E., Albano, M., Moro, M., Chini, M., Bignami, C., … Saroli, M. (2016). Uncovering deformation processes from surface displacements. *Journal of Geodynamics*, *102*, 58–82.

Swart, L. M. T. (2007). *Remote sensing voor inspectie van waterkeringen*. Nieuw-Vennep, the Netherlands: Swartvast (in Dutch).

Tarrant, O., Hambidge, C., Hollingsworth, C., Normandale, D., & Burdett, S. (2017). Identifying the signs of weakness, deterioration, and damage to flood defence infrastructure from remotely sensed data and mapped information. *Journal of Flood Risk Management*, *10*(4), 1–14.

van Baars, S. (2005). The horizontal failure mechanism of the Wilnis peat dyke. *Géotechnique*, *55*(4), 319–323.

van de Kerkhof, B., Pankratius, V., Chang, L., van Swol, R. & Hanssen, R. F. (2017). *Information extraction from dynamic PS-InSAR time series using machine learning.* AGU Fall Meeting 2017. New Orleans, USA.

van Leijen, F. J. (2014). *Persistent Scatterer Interferometry based on geodetic estimation theory.* (PhD thesis). Delft, the Netherlands: Delft University of Technology.

van Leijen, F. J., & Hanssen, R. F. (2008). *Ground water management and its consequences in Delft, the Netherlands as observed by persistent scatterer interferometry*. Frascati, Italy: FRINGE2007.

Vergouwe, R., & Sarink, H. (2014). *De veiligheid van Nederland in kaart: eindrapportage*. Den Haag, the Netherlands: Rijkswaterstaat Projectbureau VNK (in Dutch).

Zebker, H. A., & Villasenor, J. (1992). Decorrelation in interferometric radar echoes. *IEEE Transactions on Geoscience and Remote Sensing*, *30*(5), 950–959.

How to cite this article: Özer IE, van Leijen FJ, Jonkman SN, Hanssen RF. Applicability of satellite radar imaging to monitor the conditions of levees. *J Flood Risk Management*. 2018;e12509. https://doi.org/10.1111/jfr3.12509